Title: Insights in Cellular Uptake Mechanisms of pDNA – Polycationic Amphiphilic Cyclodextrin Nanoparticle (Cdplexes)

Authors: Diaz-Moscoso A., Vercauteren D., Rejman J., Benito J.M., Ortiz Mellet C., De Smedt S.C., Garcia Fernández J.M.

In: Journal of Controlled Release, 143(3), 318-325 (2010)

10.1016/j.jconrel.2010.01.016

Insights in Cellular Uptake Mechanisms of pDNA—Polycationic Amphiphilic Cyclodextrin Nanoparticles (CDplexes)

Alejandro Díaz-Moscoso,[†,¶] Dries Vercauteren,[‡,¶] Joanna Rejman,[‡] Juan M. Benito,[†] Carmen Ortiz Mellet,*[,§] Stefaan C. De Smedt,*[,‡] and José M. García Fernández*[,†]

Instituto de Investigaciones Químicas, CSIC – Universidad de Sevilla, Américo Vespucio 49, Isla de la Cartuja, E-41092 Sevilla, Spain, Departamento de Química Orgánica, Facultad de Química, Universidad de Sevilla, Apartado 1203, E-41071 Sevilla, Spain, and Laboratory of General Biochemistry and Physical Pharmacy. Department of Pharmaceutics, Gent University, Harelbekestraat 72, B-9000 Gent, Belgium.

* Corresponding authors.

[†] Instituto de Investigaciones Químicas. Tel: +34 954 489 559. Fax: 954 460 565. E-mail: jogarcia@iiq.csic.es

[‡] Gent University. Tel: +32 9 264 80 76. Fax: +32 9 264 8189. E-mail: Stefaan.Desmedt@UGent.be

[§] Universidad de Sevilla. Tel: +34 954 559 806. Fax: +34 954 624 960. E-mail: mellet@us.es

Running Title: Cellular Uptake of pDNA—Cyclodextrin Nanoparticles

[¶] A. D.-M. and D. V. have equally contributed to the reported work.

Abstract

It is generally recognized that the major obstacle to efficient gene delivery is cellular internalization and endosomal escape of the DNA. Recently, we have developed a modular strategy for the preparation of well-defined polycationic amphiphilic cyclodextrins (paCDs) capable of complexing and compacting DNA into homogeneous nanoparticles (<70 nm). Since paCDs resemble both cationic polymers and cationic lipids, it is conceivable that the corresponding pDNA-paCD nanoparticles (CDplexes) might use the cell uptake and endosomal escape mechanisms described for both lipoplexes and polyplexes. To verify this hypothesis, we have now investigated the uptake and transfection efficiencies of CDplexes in the presence of several inhibitors of endocytosis, namely chlorpromazine, genistein, dynasore and methylated β-cyclodextrin (MbCD). Our data show that CDplexes obtained from paCD **1**, which ranks among the most efficient paCD gene vectors reported up to date, are internalized by both clathrin-dependent (CDE) and clathrin-independent endocytosis (CIE), both processes being cholesterol- and dynamin-dependent. We observed that the largest fraction of gene complexes is taken up via CDE, but this fraction is less relevant for transfection. The smaller fraction that is internalized via the CIE pathway is predominantly responsible for successful transfection.

Introduction

The successful delivery of therapeutic genes into cells and their availability at the intracellular site of action are crucial requirements for successful gene therapy. During the last decade, under the advent of *nanotechnology*, a broad diversity of creative materials featuring promising properties for nonviral gene delivery applications has emerged, *(1)*. Cationic polymers and lipids, or their combinations, have shown the ability to bind nucleic acids through electrostatic interactions and condense them into complexes that can be readily internalized by cells *(2-3)*. The gene delivering capabilities of many of these systems have been thoroughly investigated. Yet, drawing firm conclusions that might serve to provide feedback for the design of improved delivery entities is a delicate issue as a consequence of the essentially polydisperse nature of such structures *(4)*.

The control of the architecture of multifunctional macromolecules is a major determinant in the rational design of successful nonviral gene delivery systems. Novel

strategies have been implemented to build up well defined constructs featuring self-assembling capabilities in the presence of nucleic acids. In this context, the unique characteristics of dendrimers and other highly ordered clusters, such as uniformity, monodispersity and multivalency, have attracted increasing attention *(5-8)*. Homogeneous external functionalization of these platforms becomes, however, exponentially more complicated as the dendrimer generation increases *(9-10)*. The use of preorganized macrocyclic scaffolds, such as calixarenes, to achieve a precise alignment of functional elements represents an interesting alternative *(11-14)*. The commercially available cyclomaltooligosaccharides (cyclodextrins; CDs) appear particularly attractive on those grounds *(15-16)*. CDs combine biocompatibility, availability, and a tubular symmetric framework with well differentiated faces that can be selectively modified in order to attain an exquisite control of the presentation and orientation of the assembled elements *(17-19)*. Chemically modified CDs have been already incorporated into polycationic polymers that can effectively complex and deliver plasmid DNA (pDNA) *(20-21)*. More recently, monodisperse polycationic CD conjugates with promising pDNA delivery capabilities were prepared by homogeneous functionalization of the CD primary rim *(22-24)*. Aiming at merging the virtues of both cationic polymers and cationic lipids in a flexible, well defined framework, we have reported a modular synthetic strategy for the preparation of polycationic amphiphilic CDs (paCDs) that allows the installation of different building blocks onto either face of the truncated-cone structure in a sequential and controlled way, offering a unique opportunity for structure-activity relationship (SAR) studies *(25-27)* (Figure 1). The pDNA complexing capabilities and *in vitro* transfection efficiencies of the corresponding pDNA-paCDs complexes (CDplexes) were found to be dependent on the CD decoration pattern. Notably, transfection efficiencies surpassing that of commercial polyethyleneimine (PEI) polymers-based polyplexes for BNL-CL2 and COS-7 cell lines were observed for some paCD representatives, such as **1** *(28)* (Figure 2). Since paCDs resemble both cationic polymers and cationic lipids, it is conceivable that the resulting pDNA-paCD nanoparticles (CDplexes) might be taken up by the cells and later released from the endosomes by mechanisms earlier described for both lipo- and polyplexes.

In eukaryotic cells the following mechanisms of endocytosis can be distinguished: phagocytosis, macropinocytosis (MP), clathrin dependent endocytosis (CDE) and clathrin independent endocytosis (CIE) *(29)*. Phagocytosis is typically restricted to specialized cells such as macrophages, whereas macropinocytosis is a constitutive bulk internalization process

typically characterized by the formation of membrane protrusions and engulfing large volumes *(30)*. CDE and CIE are the most relevant mechanisms operating in the internalization of pDNA-nonviral gene delivery system complexes. The first route is characterized by the formation of clathrin coated pits *(31)*. CIE includes several pathways which share a cholesterol dependency *(32)*, among which caveolin mediated endocytosis Cav-ME is probably the most thoroughly characterized. In this case the membrane of the formed vesicles, which are called cavicles, typically contains caveolin-1 *(33,34)*. Selective inhibition of the different internalization pathways has been shown to be a powerful tool to investigate uptake mechanisms of nanoparticles and infer the relevance of the blocked pathway in the internalization mechanism *(32,35-43)*. Previous studies have shown that lipoplexes enter the cells predominantly via CDE *(44)*. Polyplexes, however, are internalized less uniformly. Their uptake seems to occur via MP and CDE as well as CIE *(44)*. Nonetheless, it has been observed for PEI complexes that it is predominantly the fraction that is taken up via CIE that leads to gene expression *(45-47)*.

The purpose of this work was to get insight on the uptake mechanisms of pDNA-paCD nanoparticles and study whether the different internalization pathways might influence the intracellular fate of the CDplexes and their transfection efficiency. The dendritic tetradecacationic paCD **1**, for which a gram-scale synthetic procedure has been optimized, was selected for this study since it was previously shown to form small (< 70 nm) CDplexes in which pDNA was fully protected from degradation, with transfection efficiencies up to one order of magnitude higher as compared to branched PEI (25 KDa) in BNL-CL2 and COS-7 cells both in serum free and serum-containing (10%) media *(28)*. A set of selective endocytic pathway inhibitors, including chlorpromazine, genistein, dynasore and methylated β-cyclodextrin (MbCD), have been used in the present study. In addition, a fluorescently labeled (lissamine-rhodamine) derivative of paCD **1** has been synthesized to study uptake and intracellular trafficking of the CDplexes by confocal laser scanning microscopy.

Experimental Section

General Methods

Reagents and solvents were purchased from commercial sources and used without further purification, except for dichloromethane, which was distilled over CaH_2 under N_2 stream. Products **2** *(48)*, **6** *(15)* and **7** *(15)* were prepared according to literature procedures.

Optical rotations were measured at 20 ºC in 1-dm tubes. ^{1}H (and ^{13}C) NMR spectra were recorded at 500 (125.7) or 300 (75.5) MHz. 2D COSY and HMQC experiments were used to assist NMR assignments. Thin-layer chromatography (TLC) was carried out on silica-coated aluminum sheets, with visualization by UV light and by charring with 10% H_2SO_4 or 0.1% ethanolic ninhydrin. Column chromatography was carried out on silica gel (230-400 mesh). Electrospray mass spectra were obtained from samples dissolved in MeOH, MeCN, H_2O or their mixtures at low μM concentration. Ampicillin, chlorpromazine, methyl β-cyclodextrin (MbCD), genistein and dynasore were purchased from Sigma Aldrich (Bornem, Belgium). Serumfree medium OptiMEM is purchased from Invitrogen (Merelbeke, Belgium).

Heptakis[6-(2-*tert*-butoxycarbonylaminoethylthio)-6-deoxy]cyclomaltoheptaose (3). To a suspension of heptakis(6-bromo-6-deoxy)cyclomaltoheptaose *(48)* (**2**, 2.52 g, 1.59 mmol) and cesium carbonate (5.13 g, 15.6 mmol) in dry DMF (30 mL), *tert*-butyl *N*-(2-mercaptoethyl)carbamate (15.9 mmol, 1.4 eq) was added. The suspension was heated, under Ar atmosphere, at 70 ºC for 48 h. The reaction mixture was cooled to room temperature, poured into ice-water, and stirred overnight. The resulting solid was filtered, washed with a large volume of water and finally washed with a small amount of cold Et_2O. The residue was purified by column chromatography (40:10:1→ 30:10:1 CH_2Cl_2-MeOH-H_2O) to give **3** (3.04 g, 85%) having physicochemical properties identical to those previously reported *(28)*.

Heptakis[6-(2-*tert*-butoxycarbonylaminoethylthio)-6-deoxy-2,3-di-*O*-hexanoyl]cyclomaltoheptaose (4): To a solution of **3** (2.0 g, 0.89 mmol) in dry pyridine (10 mL) under Ar, DMAP (4.56 g, 37.3 mmol, 3 eq) and hexanoic anhydride (12 mL, 49.8 mmol, 4.0 eq) were added. The mixture was heated at 70 ºC for 4-5 h. Then, MeOH (10 mL) was added and the mixture was further stirred at 70 ºC for 3 h. The solvents were evaporated under reduced pressure, ice-water (50 mL) was added and extracted with CH_2Cl_2 (4 × 50 mL). The organic phase was washed with diluted sulfuric acid (2 × 50 mL) and cold aqueous saturated $NaHCO_3$ (4 × 50 mL), dried (Na_2SO_4), filtered, concentrated and purified by column chromatography (1:3 EtOAc-petroleum ether) to give **4** (2.44 g, 76%) having physicochemical properties identical to those previously reported *(28)*.

Heptakis[6-(2-aminoethylthio)-6-deoxy-2,3-di-*O*-hexanoyl]cyclomaltoheptaose Heptahydrochloride (5): Treatment of carbamate **4** (1.42 g, 0.4 mmol) with 1:2 TFA-CH_2Cl_2 (20 mL) at RT for 3 h, followed by evaporation of the solvents and freeze-drying from a

diluted HCl solution, gave pure **5** (1.20 g, 99%) as a white foam having physicochemical properties identical to those previously reported *(28)*.

2-[*Bis*[2-(*tert*-butoxycarbonylamino)ethyl]amine]ethyl Isothiocyanate (8). To a solution of 2-azidoethyl-bis[2-(*tert*-butoxycarbonylamino)ethyl]amine *(15)* (**7**, 0.72 g, 1.89 mmol) in dry dioxane (15 mL), triphenylphosphine (0.55 g, 1.1 eq, 2.1 mmol) and carbon disulfide (1.14 mL, 10 eq, 18.9 mmol) were added. The reaction mixture was stirred under N_2 atmosphere for 16 h. Then the solvent was removed under reduced pressure and the residue was purified by column chromatography using 1:2 EtOAc-petroleum ether as eluent to give **8** (0.63 g, 86 %) having physicochemical properties identical to those previously reported *(28)*.

Heptakis[6-deoxy-6-(2-(*N*'-(2-(*N*,*N*-di-(2-(*N*-*tert*-butoxycarbonylamino)ethyl)amino)ethyl)-thioureido)ethylthio)-2,3-di-*O*-hexanoyl]cyclomaltoheptaose (9). To a solution of **5** (0.48 g, 0.15 mmol) and Et_3N (0.29 mL, 2.12 mmol, 2.0 eq) in CH_2Cl_2 (5 mL), a solution of **8** (0.49 g, 1.26 mmol, 1.2 eq) in CH_2Cl_2 (5 mL) was added and the reaction mixture was stirred at RT for 3 h. The solvent was evaporated under reduced pressure and the residue was purified by column chromatography (50:1 → 20:1 CH_2Cl_2-MeOH) to give **9** (0.72 g, 85%) having physicochemical properties identical to those previously reported *(28)*.

Heptakis[6-deoxy-6-(2-(*N*'-(2-(*N*,*N*-di-(2-aminoethyl)amino)ethyl)thioureido)ethylthio)-2,3-di-*O*-hexanoyl]cyclomaltoheptaose (1). Treatment of carbamate **9** (0.6 g, 0.11 mmol) with 1:2 TFA-CH_2Cl_2 at RT for 3 h, followed by evaporation of the solvent and freeze-drying from diluted HCl solution, gave **1** (0.50 g) in quantitative yield. Its identity and purity was confirmed by ESI-MS, comparison of the corresponding ^1H and ^{13}C NMR spectra with those of an authentic sample *(28)* and combustion analysis.

Lissamine-Rhodamine Labeled paCD 10. To a solution of paCD **1** (83 mg, 17 μmol) and Et_3N (50 μL, 0.35 mmol) in freshly distilled CH_2Cl_2 (10 mL) under N_2, lissamine-rhodamine sulfonyl chloride (LRSC, 10 mg, 17 μmol) was added. The reaction was stirred at RT for 2 days in the dark. The solvents were then removed under vacuum and the residue was purified by size exclusion chromatography (Sephadex LH-20, MeOH). Lisamine-Rhodamine labeled paCD **10** was obtained as a dark red foam after liophilization from diluted HCl (73 mg, 79%). The corresponding ^1H NMR spectrum, recorded in MeOD at 313 K, featured the

characteristic aromatic signals for lissamine-rhodamine (LS) at δ 8.75, 8.24, 7.62 and 7.26-6.97 ppm, with intensities fitting the expected 1:1 LS-paCD average ratio. ESI-MS: *m/z* 1196.5 $[M\text{-}Rho + 4\ H]^{4+}$, 1061.5 $[M + 4\ H]^{4+}$, 957.3 $[M\text{-}Rho + 5\ H]^{5+}$, 848.8 $[M + 5\ H]^{5+}$.

Plasmid Preparation and Labeling.

For transfection, the luciferase encoding plasmid pGL4.13 (Promega, Leiden, The Netherlands) was used. The plasmid was transformed into the competent *E. coli* DH10b strain (Promega, Leiden, The Netherlands) according to the manufacturer's instructions. The transformed bacteria were then selected for ampicillin resistance and grown till an optical density of 1.5. The plasmid was purified with the PureLink™ HiPure Plasmid Gigaprep Kit (Invitrogen, Merelbeke, Belgium). The plasmid was re-suspended to a concentration of 1 μg μL^{-1} in TE buffer (10 mM Tris, 1 mM EDTA, pH 7.4). For uptake studies, the plasmid was labeled with the nucleic acid stain YOYO®-1 iodide (λ_{ex} = 491, λ_{em} = 509, Molecular Probes, Merelbeke, Belgium). For the labeling, 100 μg of plasmid was added to 15 nmol of YOYO-1 in 20 mM HEPES buffer for 1 h at RT, which should result in a labeling density of 1 YOYO-dye per 10 bp. The YOYO-1-DNA complexes were finally purified by an ethanol precipitation and re-suspended to 1 μg μL^{-1} in TE buffer.

Preparation of CDplexes.

To prepare complexes, plasmid DNA was mixed with polycationic amphiphilic cyclodextrins. The paCD derivative was dissolved in DMSO and diluted in water to a final stock solution of 20 $mg{\cdot}mL^{-1}$ (4.2 mM) (1:2 DMSO-water). pDNA was diluted with OptiMEM to a concentration of 0.04 μg μL^{-1} (equal to 124 μM of phosphate) and mixed with paCD derivate to yield the desired N/P ratio. The preparation was vortexed for 12 minutes before diluting it 10 times in OptiMEM. This solution was used for uptake or transfection experiments.

Cell Culture

Vero (African green monkey kidney epithelial cell line; ATCC number CCL-81) were cultured in Dulbecco's modified Eagles' medium (DMEM; Invitrogen, Merelbeke, Belgium) supplemented with 10 % fetal bovine serum (Perbio, Erembodegem, Belgium), 2 mM L-glutamine and 2 % penicillin/streptomycin (Invitrogen, Merelbeke Belgium) and grown at 37 °C in a humidified atmosphere containing 5 % CO_2.

Transfection experiments

Cells were seeded into 12-well plates (100.000 cells per well) and allowed to attach overnight. Subsequently, the culture medium was removed and CDplexes were added to the well (2 μg of DNA, N/P 10). The complexes were removed after 4 h. Luciferase activity, as well as the total cellular protein concentration, was measured after 48 h. To determine the luciferase activity, the cells were washed with PBS and lysed with 200 μL of cell culture lysis buffer (Promega, Leiden, The Netherlands) (30 min, RT). Samples were centrifuged (4 ºC, 14000 rpm, 5 min). Subsequently, luciferase activity was determined in the supernatants with the Promega luciferase assay kit (Promega, Leiden, The Netherlands) according to the manufacturer's instructions. Briefly, 100 μL of substrate solution were added to 40 μL sample in a white 96-microtiter plate and after a 2 s delay, the luminescence was measured during 10 s with the GloMax™ 96 luminometer (Promega, Leiden, The Netherlands). The protein concentration was determined with the Biorad Bradford Protein assay (Biorad, Eke, Belgium). The Biorad reagent (50 μL) was mixed with cell lysate (2 μL) and water (198 μL) in a transparent 96-microtiter plate and the absorbance was measured on a Wallac Victor2 absorbance plate reader (Perkin Elmer-Cetus Life Sciences) at 590 nm. The luciferase activity, expressed as relative light units (RLU) per μg of protein, was used as a measure for the efficiency of transfection with the CDplexes. Mean values were obtained from at least two separate experiments carried out in triplicate.

Cell Viability Assay

Cell viability was assessed with the CellTiterGlo Proliferation Assay (Promega, Leiden, The Netherlands) according to the manufacturer's instructions. Briefly, 10.000 Vero cells were seeded in a white 96-well microtiter plate with transparent bottom (Greiner Bio-One, Wemmel, Belgium). The cells were treated with 100 μL of inhibitors and/or complexes for the indicated times. Subsequently, CellTiterGlo reagent was added and incubated with the cells for 5 min till complete lysis. Cell debris was spun down and luminescence was measured in the supernatants on a GloMax™ 96 luminometer with 1 s integration time. Each experiment was performed in quadruplicate.

CDplexes Uptake Studies

Vero cells were seeded into 6-well plates (300.000 cells per well) and allowed to attach overnight. The cells were then incubated with the CDplexes, prepared with YOYO-1

labeled pDNA, in OptiMEM. The fluorescence of the non-internalized complexes, attached to the plasma membrane was quenched by a 5-minute-washing with 0.2% trypan blue (Sigma, Bornem, Belgium) in PBS solution. After washing with PBS, the cells were detached with trypsin, centrifuged and re-suspended in ice cold flow buffer. The samples were analyzed with a 5-color FC500 flow cytometer (Beckman Coulter, Nyon, Switzerland) equipped with an argon laser (λ_{ex} = 488 nm). CXP software (Beckman Coulter, Nyon, Switzerland) was used for the analysis. The internalization of CDplexes was calculated as the mean fluorescence value (average of three independent experiments). The 0% uptake was determined from cells incubated at 4 °C. The 100% uptake was determined from cells that had been incubated with the complexes without being exposed to any inhibitor.

Inhibitor Studies

Prior to incubation with CDplexes, Vero cells were pre-incubated with chlorpromazine, MbCD, genistein or dynasore prepared in OptiMEM (1 h, 37 °C). Subsequently this medium was removed and substitute with OptiMEM containing fresh inhibitor and complexes. The following stock solutions of inhibitors were used: freshly prepared 10 mg mL^{-1} chlorpromazine in water, freshly prepared 5 mM (6.6 mg mL^{-1}) MbCD in water, 50 mM genistein in DMSO (stored in the freezer), and 1 μg μL^{-1} dynasore in DMSO (stored in the freezer).

Live Cell Imaging of Fluorescently Labeled CDplexes

Vero cells were seeded at a concentration of 400.000 cells per well on sterile MatTek coverslips (1.5)-bottom dishes (MatTek Corporation, MA, USA). The cells were incubated with 2 mL of CDplexes (N/P 10, 12 μg DNA). The fluorescent CDplexes were visualized with a Nikon C1 confocal laser scanning microscope (CLSM) (Nikon Benelux, Brussels, Belgium) equipped with a Plan Apo VC 60x 1.4 NA oil immersion objective lens. Lissamine-rhodamine labeled compound (**10**) was excited with the solid state 561 nm laser line and the emitted light was collected using a 580-630 nm band pass filter. Cells were kept in a stage top incubator with controlled temperature, humidity and CO_2 pressure (Tokai Hit, Shizuoka, Japan). Representative 2D confocal images were acquired approximately through the central plane of the cell.

Results and Discussion

Synthesis

The paCD representative selected for this study (**1**) incorporates a cluster of fourteen primary amino groups that can act cooperatively with a belt of thiourea segments in the reversible complexation of the polyphosphate skeleton of plasmids through concerted electrostatic and hydrogen bonding interactions. It contains, additionally, a rim of tertiary amino groups intended to mimic the pH-regulating effect ascribed to tertiary amines in PEI polymers *(49)*. Its synthesis had previously been accomplished, though only in the 10 mg scale *(28)*. For the purpose of this work, and in view of further studies, we have scaled up the preparation of **1** to the gram scale through the reaction sequence depicted in Scheme 1. The key step is the coupling reaction of the isothiocyanate-functionalized Boc-protected polyamine dendron **8** with the βCD heptaamine scaffold **5**, in which the lipophilic hexanoyl tails have already been installed. The preparation of the heptacationic βCD precursor was effected in four steps from commercial βCD by a reaction sequence involving primary face-selective bromination with *N*-bromosuccinimide (→**2**) *(48)*, nucleophilic displacement of the halogen groups by N-Boc-protected cysteamine (→**3**), homogeneous acylation of the secondary hydroxyls with hexanoic anhydride and *N,N*-dimethylaminopyridine (DMAP) in pyridine (→**4**), and final acid-promoted hydrolysis of the carbamate groups. This synthetic route proved to be very convenient, furnishing compound **5** with analytical purity in a consistent 60% overall yield in gram scale.

The coupling reaction of isothiocyante **8** and heptaamine **5** proceeded to completion in dichloromethane in the presence of triethylamine, as monitored by TLC and ESI-MS (→**9**). After chromatographical purification, the corresponding heptathiourea adduct was isolated in 85% yield. Trifluoroacetic acid-mediated hydrolysis of the Boc protecting groups furnished the target paCD **1** in quantitative yield, which was characterized and stored as the corresponding tetradecahydrochloride salt.

In order to monitor real time cell uptake of pDNA:paCD nanoparticles by advanced light microscopy techniques, compound **1** was covalently labeled with lissamine-rhodamine. This fluorescent probe offers chemical stability and strong fluorescence intensity over a wide range of conditions (pH and ionic strength) and can be easily installed on amine-bearing

macromolecules. Thus, compound **1** was reacted with lissamine-rhodamine sulfonyl chloride (LRSC) in CH_2Cl_2 in equimolecular relative proportion, in order to obtain an average incorporation of one fluorescent probe per paCD molecule (Scheme 2). The resulting lissamine-rhodamine labeled paCD (**10**) was finally purified by size-exclusion chromatography. Compounds **1** and **10** (and their combined formulations) featured comparable self assembling capabilities in the presence of plasmids. Fluorescence of **10**, though less intense than LRSC, proved to be sufficient for imaging requirements. Maximum fluorescence intensity of **10** (λ_{em} 595 nm) was achieved at a concentration of 25 μM in water. Above this concentration, larger aggregates might be formed and self-quench fluorescence might occur.

Uptake Kinetics of CDplexes

We have previously reported that paCD **1** efficiently complexes plasmid DNA (pDNA) forming positively charged particles (65 nm mean hydrodynamic diameter, ζ-potential +40 mV at N/P 10) *(28)*. Transfection experiments with the newly prepared **1**:pDNA (pCMV-Luc) on HeLa cells indicated that maximum transfection efficiency occurred at N/P 5 (Figure 3). Interestingly, transfection mediated by these CDplexes was only slightly affected by the presence of serum, known to be a major limitation for efficient application of cationic carriers (Figure 3A). As expected, expression of the luciferase gene decreased over the time, though enzyme activity was still detectable at day 10 when the experiment was concluded (Figure 3B).

The uptake kinetics of the CDplexes by Vero cells, using YOYO-1 labeled DNA, is presented in Figure 4. After 1 h-incubation the CDplexes were taken up by the entire population of the cells. The mean fluorescence, shown in the white bars, gradually increased till it reached a plateau after 3 h. Longer incubation times did not result in further increase of cell associated fluorescence. These data indicate that 2-h-incubation should be sufficient for efficient uptake of CDplexes by cells.

Uptake of CDplexes was also monitored by confocal microscopy using the fluorescently labeled paCD **10**. Snapshots at different time points are presented in Figure 5. Fluorescently-labeled CDplexes were internalized already 40 min after adding them to the cells (Figure 5A). The amount of intracellular CDplexes increased over the time, as shown in Figures 5B and C, and tended to accumulated in the vicinity of the nucleus. The complexes could be still detected intracellularly after 48 h (Figure 5D).

In some micrographs, large CDplex particles are visible outside the cell (Figure 5A), indicating that either paCD-pDNA complexes or paCD particles alone can aggregate in the extracellular milieu. Another interesting feature is the absence of accumulation of CDplexes or paCDs at the cellular membrane, ruling out the possibility of irreversible hydrophobic interactions between membrane lipids and the hydrocarbon tails of CDs. It is conceivable that in order to shield from the polar environment, hydrocarbon chains are oriented towards the inner core of the CDplex, which limits their interaction with plasma membrane lipids.

Endocytosis of CDplexes in the Presence of Inhibitors

To gain inside into the relative contribution of the different endocytotic pathways in CDplex-mediated transfection, four endocytosis inhibitors were applied: (i) genistein, a tyrosine-kinase inhibitor that causes local disruption of the actin network at the site of endocytosis and inhibits the recruitment of dynamin II, both known to be indispensable events in the caveolae-mediated uptake mechanism *(50,51)*; (ii) dynasore, an inhibitor that blocks dynamin activity, disturbing the pinching off of newly formed vesicles, a process that is known to be essential for at least CDE *(52)*; (iii) chlorpromazine, a cationic amphiphilic drug which is believed to inhibit clathrin-coated pit formation by a reversible translocation of clathrin and its adapter proteins from the plasma membrane to intracellular vesicles *(53)*, and (iv) methyl β-cyclodextrin (MbCD), a randomly methylated cyclomaltoheptaose derivative that inhibits cholesterol-dependent endocytic processes by reversibly extracting the steroid out of the plasma membrane *(54)*.

To establish an optimal protocol for the use of the inhibitors, cell viability in their presence was first determined. Different concentrations of each inhibitor were tested in the absence and in the presence of CDplexes prepared at two different N/P ratios (5 and 10). Cellular toxicity was assessed with the CellTiterGlo cell viability test. The results are shown in Figure 6.

Genistein alone showed limited toxicity towards Vero cells after 5 h incubation. The highest concentration tested (400 mM) reduced viability by less than 20% (Figure 6A). Incubation in the presence of genistein and CDplexes turned out to increase toxicity, especially at the higher N/P ratio (26% and 75% viability decrease for N/P 5 and 10, respectively). Dynasore (20-50 μM) displayed only moderate toxicity on Vero cells (Figure 6B). At the highest concentration (50 μM), viability was lowered by 20% only. In combination with CDplexes, cell viability decreased by around 10% and 40% for N/P 5 and

10, respectively. Remarkably, increasing dynasore concentrations apparently protected Vero cells from paCDs-induced toxicity, possibly due to an efficient endocytosis blocking effect (see below). Vero cells were virtually insensitive to chlorpromazine up to 10 μg mL^{-1} for 5 h. Higher concentrations, on the other hand, led to 100% cell death (Figure 6C). Chlorpromazine at 10 mg mL^{-1}, in combination with CDplexes (N/P 10), reduced cell viability by as much as 70%. Treatment with MbCD caused cytotoxicity at concentrations higher than 7.5 mM (Figure 6D), while combined incubation with MbCD (5 mM) and CDplexes (N/P 10) resulted in 50% cell viability.

Inhibitor concentrations for further transfection experiments were selected based on the toxicity assays described above. Thus, Vero cells were preincubated for 1 h with 400 μM genistein, 50 μM dynasore, 10 μg mL^{-1} chlorpromazine or with 5 mM MbCD. Next, the cells were incubated for 2 h with the YOYO-1 labeled CDplexes in the presence of the corresponding inhibitor. Figure 7 shows that after treatment with genistein, chlorpromazine and MbCD, CDplexes still were internalized by almost all the cells, albeit in lower amount. MbCD and chlorpromazine reduced the average cellular uptake of gene complexes by 80%, while genistein lowered the cellular uptake of the CDplexes only by 50%. In contrast, the uptake of the CDplexes was almost completely inhibited by dynasore. This would indicate that the uptake of CDplexes by Vero cells is strongly dependent on dynamin activity, but a large fraction of uptake is also dependent on the presence of cholesterol in the plasma membrane and the availability of clathrin at the cytoplasmic side of the plasma membrane. Furthermore, considering the efficient inhibition of CDplex uptake in the presence of chlorpromazine, known to block clathrin coated pit formation *(53)*, we can conclude that CDE probably is a major route for CDplex internalization in Vero cells. However, the fact that genistein, known to interfere with internalization via caveolae *(50)*, partially inhibited CDplex uptake does not rule out CIE routes, even if the fraction of the complexes that enter Vero cells via CDE seems to be larger than the fraction that enters via CIE.

In addition to the effect of inhibitors on the uptake of complexes we measured their effect on transfection efficiency by assaying luciferase activity 48 h after transfection (Figure 8). Genistein appeared to completely inhibit luciferase expression at 400 μM. Also dynasore inhibited transfection very efficiently at 50 μM. In the case of chlorpromazine, transfection efficiency was reduced by 50% at 10 μg mL^{-1}. No luciferase activity was measured at higher chlorpromazine concentrations, although this is probably due to the cytotoxic combination of

chlorpromazine (> 10 μg mL^{-1}) and CDplexes that resulted in almost 100% cell death (see above). In case of MbCD, concentrations of 5 mM or higher resulted in more than 80% decrease of reporter gene expression.

Conclusions

Our results demonstrate that CDplex-mediated transfection is a complex process simultaneously involving several cellular uptake mechanisms. Chlorpromazine, an inhibitor of CDE, although decreasing internalization by 76%, only partially inhibited transfection. This indicates that the small fraction that is internalized via CIE (24%) is still able to bring about moderate transfection, thus reducing the relevance of CDE route for CDplex-mediated transfection. This result is supported by the fact that genistein, an inhibitor of CIE, although reducing CDplex uptake by 50% only, completely abolished luciferase expression, pointing to the inefficiency of clathrin-coated endosomes to deliver the pDNA functionally to its target. Possibly, in this case the cargo cannot escape from the endosomes and is ultimately degraded in lysosomal compartments. These findings are in agreement with former studies on the internalization of polyplexes *(45-47)*. It must be emphasized, however, that the present observations and conclusions cannot be generalized or extrapolated to other types of DNA-paCD complexes or even other cell lines. The whole process of uptake, processing and gene expression is strongly dependent on the carrier as well as cell type and therefore should be specifically studied in a case-to-case manner.

Acknowledgements

This work was supported by the Spanish Ministerio de Innovación y Ciencia (MICINN, contract numbers CTQ2006-15515-C02-01/BQU and CTQ2007-61180/PPQ) and the Junta de Andalucía (P06-FQM-01601 and P07-FQM-2774). ADM is grateful to the CSIC for a pre-doctoral fellowship. DV is a doctoral fellow of the Institute for the Promotion of Innovation through Science and Technology in Flanders (IWT), Belgium. We gratefully acknowledge the European Commission for funding through the Integrated 6th Framework Programme MediTrans.

Supporting Information Available: NMR spectra of compounds **1**, **3-5** and **8-10**. This material is available free of charge via the Internet at http://pubs.acs.org.

References

(1) El-Aneed, A. (2004) An overview of current delivery systems in cancer gene therapy. *J. Control. Rel. 94*, 1-14.

(2) Putnam, D. (2006) Polymers for gene delivery across length scales. *Nat. Mater. 5*, 439-451.

(3) Merdan, T., Kopecek, J., and Kissel, T. (2002) Prospects for cationic polymers in gene and oligonucleotide therapy against cancer. *Adv. Drug Delivery Rev. 54*, 715-758.

(4) De Smedt, S. C., Demeester, J., and Hennink, W. E. (2000) Cationic polymer based gene delivery systems. *Pharm. Res. 17*, 113-126.

(5) Cloninger, M. J. (2002) Biological application of dendrimers. *Curr. Opin. Chem. Biol. 6*, 742-748.

(6) Svenson, S. and Tomalia, D. A. (2005) Dendrimers in biomedical applications − Reflections on the field. *Adv. Drug Deliv. Rev. 57*, 2106-2129.

(7) Lee, C. C., MacKay, J. A.: Fréchet, J. M. J., and Szoka, Jr, F. C. (2005) Designing dendrimers for biological applications. *Nat. Biotechnol. 23*, 1517-1526.

(8) Guillot-Nieckowski, M., Eisler, S., and Diederich, F. (2007) Dendritic vectors for gene transfection. *New J. Chem. 31*, 1111-1127.

(9) Kim, Y., Klutz, A. M., Kenneth A., and Jacobson K. A. (2008) Systematic investigation of polyamidoamine dendrimers surface-modified with poly(ethylene glycol) for drug delivery applications: synthesis, characterization, and evaluation of cytotoxicity. *Bioconjugate Chem. 19*, 1660-1672.

(10) Lee, J. H., Lim, Y.-B., Choi, J. S., Lee, Y., Kim, T.-I., Kim, H. J., Yoon, J. K., Kim, K., and Park, J.-S. (2003) Polyplexes assembled with internally quaternized PAMAM-OH dendrimer and plasmid DNA have a neutral surface and gene delivery potency. *Bioconjugate Chem. 14*, 1214-1221.

(11) Baldini, L., Casnati, A., Sansone, F., and Ungaro, R. (2007) Calixarene-based multivalent ligands. *Chem. Soc. Rev. 36*, 254-266.

(12) Bagnacani, V.; Sansone, F.; Donofrio, G.; Baldini, L.; Casnati, A.; Ungaro, R. (2008) Macrocyclic Nonviral Vectors: High Cell Transfection Efficiency and Low Toxicity in a Lower Rim Guanidinium Calix[4]arene. *Org. Lett. 10*, 3953-3956.

(13) Sansone, F.; Dudic, M.; Donofrio, G.; Rivetti, C.¸ Baldini, L.; Casnati, A.; Cellai, S.; Ungaro, R. (2006) DNA Condensation and Cell Transfection Properties of Guanidinium Calixarenes: Dependence on Macrocycle Lipophilicity, Size, and Conformation. *J. Am. Chem. Soc. 128*, 14528-14536.

(14) Aoyama, Y. (2004). Macrocyclic glycoclusters: from amphiphile through nanoparticles to glycoviruses. *Chem. Eur. J. 10*, 588–593.

(15) Benito, J. M., Gómez-García, M., Ortiz Mellet, C., Baussanne, I., Defaye, J., and García Fernández, J. M. (2004) Optimizing Saccharide-Directed Molecular Delivery to Biological

Receptors: Design, synthesis and biological evaluation of glycodendrimer-cyclodextrin conjugates. *J. Am. Chem. Soc. 126*, 10355-10363.

(16) Gómez-García, M., Benito, J. M., Rodríguez-Lucena, D., Yu, J.-X., Chmurski, K., Ortiz Mellet, C., Gutiérrez-Gallego, R., Maestre, A., Defaye, J., and García Fernández, J. M. (2005) Probing secondary carbohydrate-protein interactions with highly dense cyclodextrin-centered heteroglycoclusters: The *Heterocluster Effect*. *J. Am. Chem. Soc. 127*, 7970-7971.

(17) Vargas-Berenguel, A., Ortega-Caballero, F., and Casas-Solva, J. M. (2007) Supramolecular chemistry of carbohydrate clusters with cores having guest binding abilities. *Mini-Rev. Org. Chem. 4*, 1-14.

(18) Villalonga, R., Cao, R., and Fragoso, A. (2007) Supramolecular chemistry of cyclodextrins in enzyme technology. *Chem. Rev. 107*, 3088-3116.

(19) García Fernández, J. M., Ortiz Mellet, C., and Defaye, J. (2006) Glyconanocavities: Cyclodextrins and beyond. *J. Incl. Phenom. Macrocycl. Chem. 56*, 149-159.

(20) Davis, M. E., and Brewster, M. E. (2004) Cyclodextrin-based pharmaceutics: past, present and future. *Nat. Rev. Drug. Discov. 3*, 1023-1035.

(21) Heidel, J. D., Yu, Z., Liu, J. Y.-C., Rele, S. M., Liang, Y., Zeidan, R. K., Kornbrust, D. J., and Davis, M. E. (2007) Administration in non-human primates of escalating intravenous doses of targeted nanoparticles containing ribonucleotide reductase subunit M2 siRNA. *Proc. Nat. Acad. Sci. USA 104*, 5715-5721.

(22) Mourtzis, N., Paravatou, M., Mavridis, I. M., Roberts, M. L., and Yannakopoulou, K. (2008) Synthesis, characterization, and remarkable biological properties of cyclodextrins bearing guanidinoalkylamino and aminoalkylamino groups on their primary side. *Chem. Eur. J. 14*, 4188-4200.

(23) Mourtzis, N., Eliadou, K., Aggelidou, C., Sophianopoulou, V., Mavridis, I. M., and Yannakopoulou, K. (2007) Per(6-guanidino-6-deoxy)cyclodextrins: synthesis, characterisation and binding behaviour toward selected small molecules and DNA. *Org. Biomol. Chem. 5*, 125-131.

(24) Srinivasacchari, S., Fichter, K. M., and Reineke, T. M. (2008) Polycationic β-cyclodextrin "click clusters": monodisperse and versatile scaffolds for nucleic acid delivery. *J. Am. Chem. Soc.*, *130*, 4618-4627.

(25) Díaz-Moscoso, A., Balbuena, P., Gómez-García, M., Ortiz Mellet, C., Benito, J. M., Le Gourriérec, L., Di Giorgio, C., Vierling, P., Mazzaglia, A., Micalli, N., Defaye, J., and García Fernández, J. M. (2008) Rational design of cationic cyclooligosaccharides as efficient gene delivery systems. *Chem. Commun.* 2001-2003.

(26) Ortega-Caballero, F., Ortiz Mellet, C., Le Gourriérec, L., Guilloteau, N., Di Giorgio, C., Pierre Vierling, P., Defaye, J., and García Fernández, J. M. (2008) Tailoring β-cyclodextrin for DNA complexation and delivery by homogeneous functionalization at the secondary face. *Org. Lett. 10*, 5143-5146.

(27) Méndez-Ardoy, A., Gómez-García, M., Ortiz Mellet, C., Girón-González, M. D., Sevillano-Tripero, M., Salto-González, R., Santoyo-González, F., and García Fernández, J.

M. (2009) Design of macromolecular gene delivery systems by preorganization of functional elements onto a cyclodextrin scaffold: amphiphilic β-cyclodextrin “click clusters”. *Org. Biomol. Chem. 7*, 2681-2684.

(28) Díaz-Moscoso, A., Gómez-García, M., Balbuena, P., Ortiz Mellet, C., Benito, J. M., Le Gourriérec, L., Di Giorgio, C., Vierling, P., Defaye, J., and García Fernández, J. M. (2009) Polycationic amphiphilic cyclodextrin-scaffolded monodisperse gene delivery systems. *Chem. Eur. J.* in press.

(29) Conner, S. D., and Schmid S. L. (2003) Regulated portals of entry into the cell. *Nature 422*, 37-44.

(30) Kerr, M. C., and Teasdale, R. D. (2009) Defining macropinocytosis. *Traffic 10*, 364-371.

(31) Maxfield, F. R., and McGraw T. E. (2004) Endocytic recycling. *Nature Rev. Mol. Cell Biol. 5*, 121-132.

(32) Mayor, S., and Pagano, R. E. (2007) Pathways of clathrin-independent endocytosis. *Nature Rev. Mol. Cell Biol. 8*, 603-612.

(33) Pelkmans, L., Kartenbeck, J., and Helenius. A, (2001) Caveolar endocytosis of simian virus 40 reveals a new two-step vesicular-transport pathway to the ER. *Nature Cell Biol. 3*, 473-483.

(34) Sharma, D. K., Choudhury, A., Singh, R. D., Wheatley, C. L., Marks, D. L., and Pagano, R. E. (2003) Glycosphingolipids internalized via caveolar-related endocytosis rapidly merge with the clathrin pathway in early endosomes and form microdomains for recycling. *J. Biol. Chem. 278*, 7564-7572.

(35) Damke, H., Baba, T., Warnock, D. E., and Schmid, S. L. (1994) Induction of mutant dynamin specifically blocks endocytic coated vesicle formation. *J. Cell Biol. 127*, 915-934.

(36) Liu, S. H., Marks, M. S., and Brodsky, F. M. (1998) A dominant-negative clathrin mutant differentially affects trafficking of molecules with distinct sorting motifs in the class II major histocompatibility complex (MHC) pathway. *J. Cell Biol. 140*, 1023-1037.

(37) Benmerah, A., Bayrou, M., Cerf-Bensussan, N., and Dautry-Varsat, A. (1999) Inhibition of clathrin-coated pit assembly by an Eps15 mutant. *J. Cell Sci. 112*, 1303-1311.

(38) Nichols, B. J. (2002) A distinct class of endosome mediates clathrin-independent endocytosis to the golgi complex. *Nature Cell Biol. 4*, 374-378.

(39) Hinrichsen, L., Harborth, J., Andrees, L., Weber, K., and Ungewickell, E. J. (2003) Effect of clathrin heavy chain- and alpha -adaptin specific small interfering RNAs on endocytic accessory proteins and receptor trafficking in HeLa cells. *J. Biol. Chem. 278*, 45160-45170.

(40) Huang, F. T., Khvorova, A., Marshall, W., and Sorkin, A. (2004) Analysis of clathrin-mediated endocytosis of epidermal growth factor receptor by RNA interference. *J. Biol. Chem. 279*, 16657-16661.

(41) Vanden Broeck, D., and De Wolf, M. J. S. (2006) Selective blocking of clathrin-mediated endocytosis by RNA interference: Epsin as target protein. *Biotechniques 41*, 475-484.

(42) Ivanov, A. I. (2008) Pharmacological inhibition of endocytic pathways: Is it specific enough to be useful?. *Exocytosis and endocytosis* (Ivanov, A. I., Ed.) pp 15-33, Humana Press, Totowa.

(43) Vercauteren, D. N. E., Vandenbroucke, R. E., Demeester, J., De Smedt, S. C., Braeckmans, K., and Sanders, N. N. (2008) The use of endocytic inhibitors to study uptake of gene garriers. *J. Control. Rel. 132*, e17-e18.

(44) Midoux, P., Breuzard, G., Gomez, J. P., and Pichon, C. (2008) Polymer-based gene delivery: A current review on the uptake and intracellular trafficking of polyplexes. *Current Gene Ther. 8*, 335-352.

(45) Gonçalves, C., Mennesson, E., Fuchs, R., Gorvel, J. P., Midoux, P., and Pichon, C. (2004) Macropinocytosis of polyplexes and recycling of plasmid via the clathrin-dependent pathway impair the transfection efficiency of human hepatocarcinoma cells[Ast]. *Mol. Ther. 10*, 373-385.

(46) Rejman, J., Bragonzi, A., and Conese, M. (2005) Role of clathrin- and caveolae-mediated endocytosis in gene transfer mediated by lipo- and polyplexes. *Mol. Ther. 12*, 468-474.

(47) von Gersdorff, K., Sanders, N. N., Vandenbroucke, R., De Smedt, S. C., Wagner, E., and Ogris, M. (2006) The internalization route resulting in successful gene expression depends on polyethylenimine both cell line and polyplex type. *Mol. Ther. 14*, 745-753.

(48) Gadelle, A., and Defaye, J. (1991) Selective halogenation at primary positions of cyclomaltooligosaccharides and a synthesis of per-3,6-anhydro cyclomaltooligosaccharide. *Angew. Chem. Int. Ed. 30*, 78-80.

(49) Boussif, O., Lezoualc'h, F., Zanta, M. A., Mergny, M. D., Scherman, D., Demeneix, B., and Behr, J.-P. (1995) A versatile vector for gene and oliginucleotide transfer into cells in culture and in-vivo – polyethylenimine. *Proc. Nat. Acad. Sci. USA 92*, 7297-7301.

(50) Parton, R. G., Joggerst, B., and Simons, K. (1994) Regulated internalization of caveolae. *J. Cell Biol. 127*, 1199-1215.

(51) Orlandi, P. A., and Fishman, P. H. (1998) Filipin-dependent inhibition of cholera toxin: Evidence for toxin internalization and activation through caveolae-like domains. *J. Cell Biol. 141*, 905-915.

(52) Macia, E., Ehrlich, M., Massol, R., Boucrot, E., Brunner, C., and Kirchhausen, T. (2006) Dynasore, a cell-permeable inhibitor of dynamin. *Developmental Cell 10*, 839-850.

(53) Wang, L. H., Rothberg, K. G., and Anderson, R. G. (1993) Mis-assembly of clathrin lattices on endosomes reveals a regulatory switch for coated pit formation. *J. Cell Biol. 123*, 1107-1117.

(54) Rodal, S. K., Skretting, G., Garred, O., Vilhardt, F., van Deurs, B., and Sandvig, K. (1999) Extraction of cholesterol with methyl-β-cyclodextrin perturbs formation of clathrin-coated endocytic vesicles. *Mol. Biol. Cell 10*, 961-974.

Figures

Scheme 1. Convergent Synthesis of Polyaminothioureido Amphiphilic βCD (paCD) **1**.

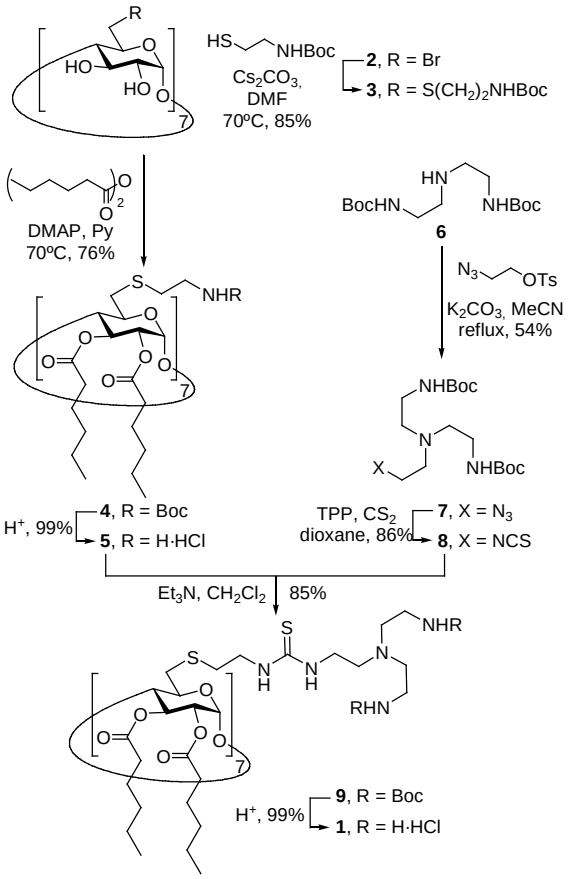

Scheme 2. Statistical Labeling of paCD **1** with Lissamine-Rhodamine Sulfonyl Chloride (LRSC).

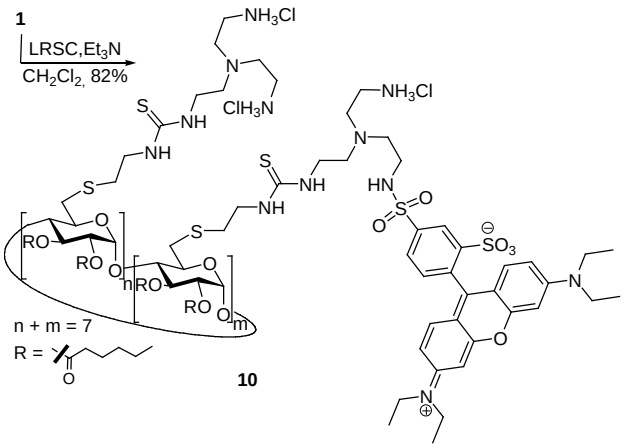

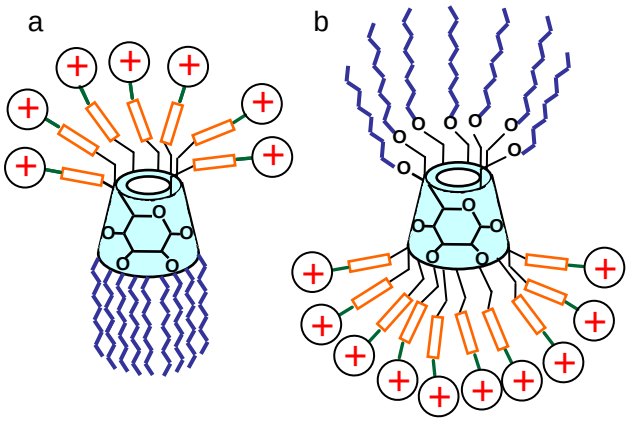

Figure 1. Schematic Representation of (a) “skirt” and (b) “jelly-fish” type Polycationic Amphiphilic CDs (paCDs). The central light-blue platform represents the cyclodextrin core, the blue weaving lines account for hydrophobic chains, the orange rectangular boxes indicate the presence of spacer elements and the encircled + signs stand for the positively charged groups.

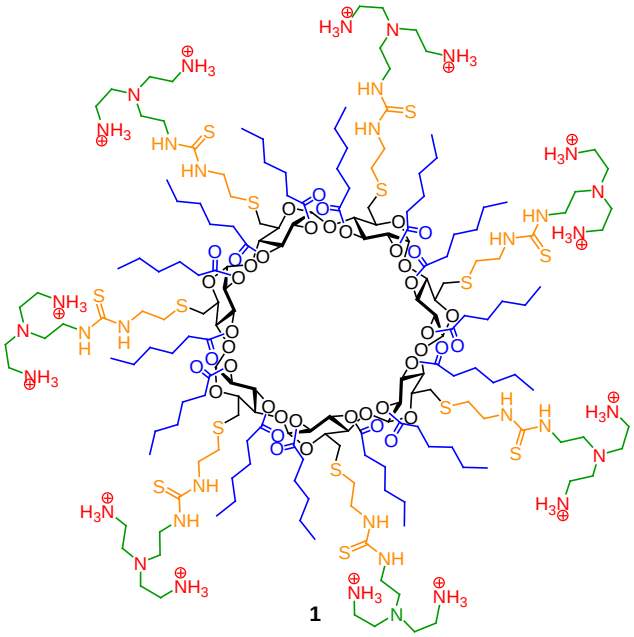

Figure 2. Chemical structure of Polyaminothioureido Amphiphilic βCD **1** (colors were selected to match Figure 1 encoding).

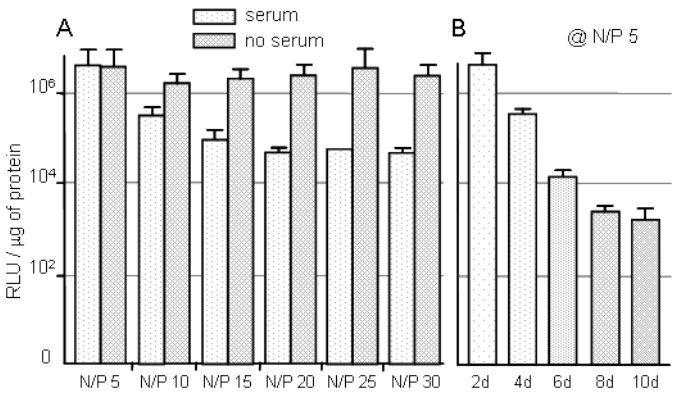

Figure 3. In vitro transfection efficiency of pDNA:paCD nanoparticles in HeLa cells (a) in the presence and in the absence of serum (10%), and (b) over the time.

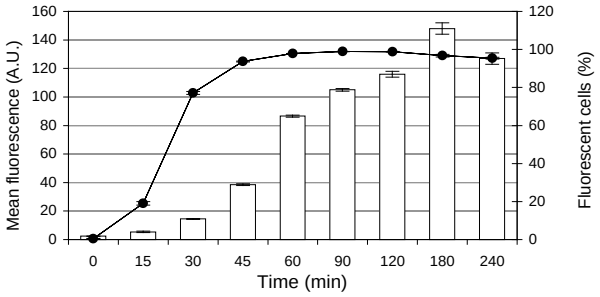

Figure 4. Uptake kinetics of YOYO-1 labeled pDNA:**1** CDplexes in Vero cells. Average cell fluorescence (A.U., bars) and amount of significantly fluorescent cells (%, dots) at the indicated time-point. The internalization was quantified with flow cytometry.

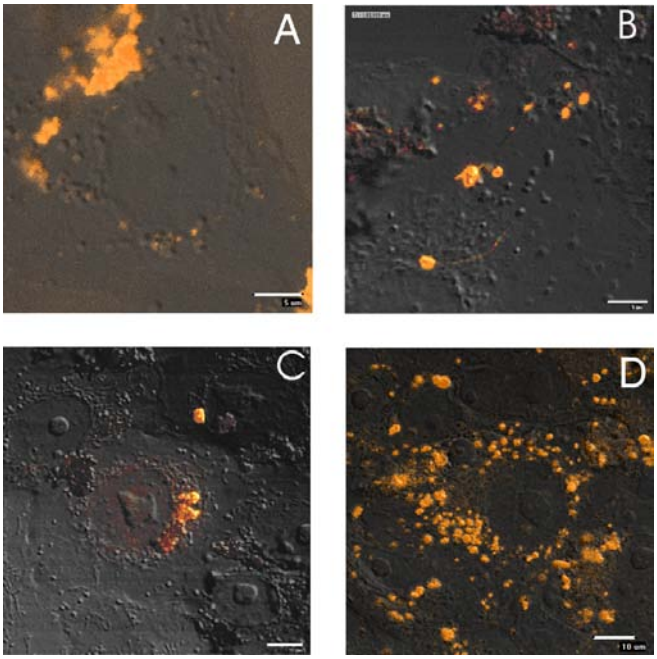

Figure 5. Confocal micrographs of the internalization of CDplexes in living Vero cells during 48 h post–transfection period (A, 40 min; B, 120 min; C, 150 min; D, 2 days).

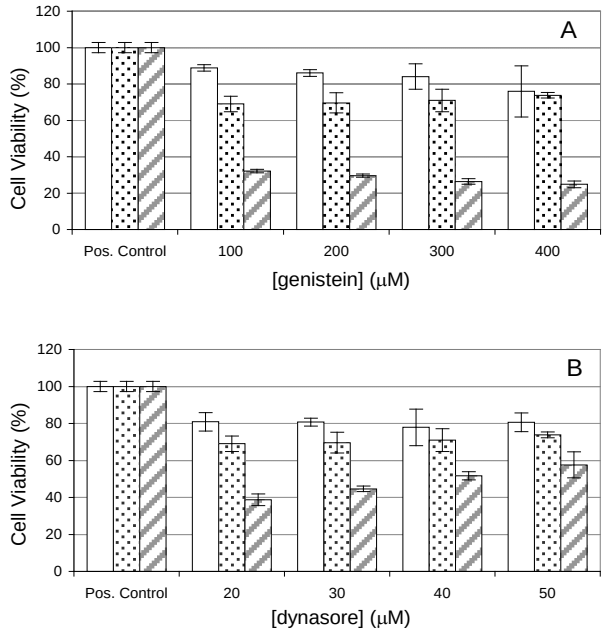

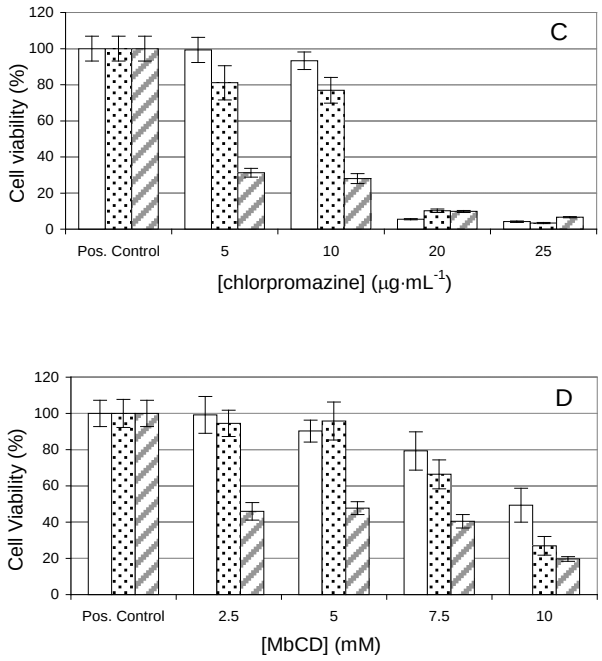

Figure 6. Viability of Vero cells incubated for 5 h with the inhibitors (white bars) or a mixture of the inhibitors and CDplexes at N/P 5 (dotted bars) and 10 (hatched bars). A, genistein; B, dynasore; C, chlorproazine; D, MbCD.

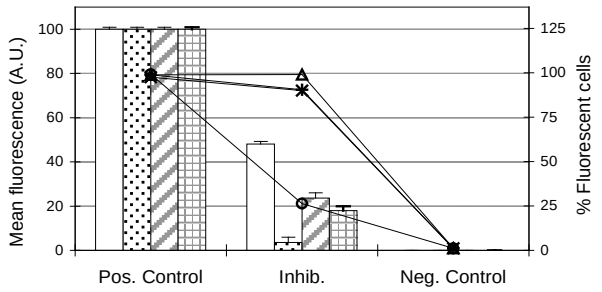

Figure 7. Effect of inhibitors on internalization of CDplexes. Vero cells were pretreated with the inhibitors for 1 h. Subsequently, fluorescently labeled CDplexes were added and incubated with the cells in the presence of inhibitors for 2 h (400 μM genistein, white bars and Δ; 50 μM dynasore, dotted bars and ○; 10 μg mL^{-1} chlorpromazine, hatched bars and +; 5 mM MbCD, cross-hatched bars and ×.

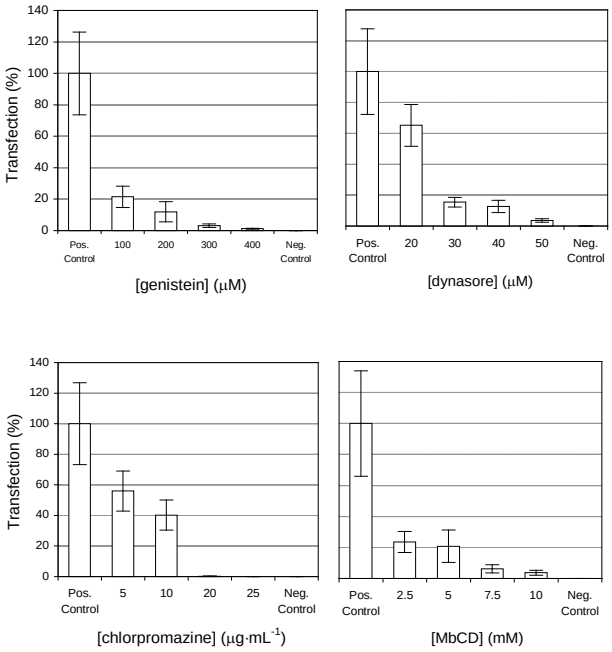

Figure 8. *In vitro* transfection efficiencies of CDplexes (N/P 10) in Vero cells in the presence of the indicated inhibitor.